

STABILITY ANALYSIS OF FAST NUMERICAL METHODS FOR VOLTERRA INTEGRAL EQUATIONS*

G. CAPOBIANCO[†], D. CONTE[‡], I. DEL PRETE[§], AND E. RUSSO[§]

Abstract. In this paper the stability properties of fast numerical methods for Volterra integral equations of Hammerstein type with respect to significant test equations are investigated.

Key words. fast numerical methods, Volterra Runge-Kutta methods, collocation methods, numerical stability

AMS subject classifications. 65R20, 45D05, 44A35, 44A10

1. Introduction. Nonlinear Volterra Integral Equations (VIEs) of Hammerstein type,

$$(1.1) \quad y(t) = f(t) + \int_0^t k(t-\tau)g(\tau, y(\tau))d\tau, \quad t \in I := [0, T], \quad y, f, k \in \mathbb{R},$$

where functions f and k are continuous on I and g satisfies the Lipschitz condition with respect to y , are the mathematical model of many problems of applied sciences. In physics, chemistry, engineering, biology, and medicine there are several problems that describe evolutionary phenomena incorporating memory ([7] and [9] and the related bibliography) whose mathematical models lead to (1.1).

It is known that the numerical treatment of VIEs has a very high computational cost: the implementation over N time steps of a classical numerical method to solve (1.1) requires a computational cost of $O(N^2)$ in time and $O(N)$ in space.

In [6] we constructed a class of Fast Collocation methods (FCOLL methods) and in [4] two classes of Fast Runge Kutta methods (FVRK methods), explicit methods of Pouzet type (FPVRK methods) and implicit methods of De Hoog and Weiss type (FHVRK methods), with the aim of using the Laplace transform of the kernel in order to reduce the computational cost of classical methods for VIEs. Among the existing inverse Laplace transform approximation techniques [12, 10, 9, 8, 13, 14, 15], FCOLL and FVRK methods are based on the idea introduced by Lubich and Schädle in [9], which is an improvement of Talbot's approximation [10, 12]. The use of this formula, permits us to reduce the computational cost to $O(N \log N)$ in time and $O(\log N)$ in space and have an high order of accuracy.

In this work we analyze the stability properties of these classes of fast methods. In Section 2 we describe briefly the Fast Collocation and the Fast Runge Kutta methods. In Sections 3 and 4, we report the stability analysis of both classes of fast methods. We study the stability properties of the fast methods with respect to test equations usually employed in the literature for stability analysis (see, for example, [1, 5] and their references), namely, the basic test equation (Section 3) and the convolution test equation (Section 4). In particular, we prove that the FCOLL and FVRK methods, when applied to both classes of test equations are stable, if they satisfy a condition which involves the coefficients of the methods and the number $M = 2N_p + 1$ of points chosen on the Talbot contour. For fixed M , we find the stability

*Received December 7, 2007. Accepted for publication July 9, 2008. Published online on November 21, 2008. Recommended by K. Burrage.

[†]Dipartimento S.T.A.T., Università degli Studi del Molise, Contrada Fonte Lappone, I-86090 Pesche (IS), Italy (giovanni.capobianco@unimol.it).

[‡]Dipartimento di Matematica e Informatica, Università di Salerno, via Ponte Don Melillo I-84084 Fisciano (SA), Italy (dajconte@unisa.it).

[§]Dipartimento di Matematica e Applicazioni "R. Caccioppoli", Università degli Studi Napoli "Federico II", Via Cintia, Monte S. Angelo I-80126 Napoli, Italy ([ida.delprete](mailto:ida.delprete@unina.it), [elvrusso](mailto:elvrusso@unina.it)).

matrix for both classes of methods and we determine a condition that provides methods with unbounded stability regions. In Section 5, we trace the stability plots for some fast methods and compare their stability regions with those of the respective classical methods. Moreover, we also report some experimental tests on a class of nonlinear problems, and we show, in our figures and tables, that they confirm the theoretical results.

2. Fast numerical methods for VIEs. Since we are interested in the linear stability analysis of fast methods, we recall the formulation of the methods when applied to the linear VIE,

$$(2.1) \quad y(t) = f(t) + \int_0^t k(t-\tau)y(\tau)d\tau, \quad t \in I := [0, T].$$

Let us discretize the interval I by introducing a uniform mesh,

$$I_h = \{t_n := nh, n = 0, \dots, N, h \geq 0, Nh = T\}.$$

The equation (2.1) can be rewritten, by relating it to this mesh, as

$$y(t) = F_n(t) + \Phi_n(t), \quad t \in [t_n, T],$$

where

$$(2.2) \quad F_n(t) := f(t) + \int_0^{t_n} k(t-\tau)y(\tau)d\tau$$

and

$$\Phi_n(t) := \int_{t_n}^t k(t-\tau)y(\tau)d\tau$$

represent respectively the *lag term* and the *increment function*. The basic idea of FCOLL and FVRK methods is to express the kernel by means of the inverse Laplace transform approximation formula introduced in [9] in order to improve Talbot's approximation [10, 12] on large intervals. The idea proposed in [9] is to split a large interval into a sequence of subintervals and in each subinterval to suitably use Talbot's approximation formula. More precisely, the interval $I = [0, T]$ is split into a sequence of fast growing intervals,

$$I_0 = [0, h], \quad I_l = [B^{l-1}h, (2B^l - 1)h], \quad l = 1, \dots, L,$$

where $B > 1$ is a fixed integer and $(2B^L - 1)h \geq T$. The chosen Talbot contour Γ_l associated to each subinterval I_l is parametrized by

$$(2.3) \quad \begin{aligned} (-\pi, \pi) &\rightarrow \Gamma_l \\ \vartheta &\rightarrow \gamma_l(\vartheta) = \sigma + \mu_l(\vartheta \cot(\vartheta) + i\nu\vartheta). \end{aligned}$$

Such a contour is determined by opportunely choosing the geometrical parameters σ, μ_l and ν , which are such that all the singularities of the Laplace transform $K(s)$ of the kernel $k(t)$ lie to the left of the contour. The approximation of the kernel $k(t)$ on the interval I_l results from applying the trapezoidal rule on the Talbot's contour Γ_l ,

$$(2.4) \quad k(t) = \frac{1}{2\pi i} \int_{\Gamma_l} K(\lambda)e^{t\lambda}d\lambda \approx \sum_{j=-N_p}^{N_p} \omega_j^{(l)} K(\lambda_j^{(l)}) e^{t\lambda_j^{(l)}}, \quad t \in I_l,$$

where

$$\omega_j^{(l)} = -\frac{i}{2(N+1)}\gamma_l'(\vartheta_j), \quad \lambda_j^{(l)} = \gamma_l(\vartheta_j), \quad \vartheta_j = \frac{j\pi}{N+1}.$$

The number of quadrature points $M = 2N_p + 1$ chosen on Γ_l is independent of l and it is much smaller than would be required for a uniform approximation on the whole interval I [9].

The resulting error satisfies [9, 10]

$$(2.5) \quad \|E(t)\|_{t \in I} = O(e^{-c\sqrt{M}}),$$

for $M \rightarrow \infty$, uniformly on I , where the positive constant c depends on the distance of the singularities of the Laplace transform $K(s)$ of the kernel $k(t)$ with respect to the Talbot contour. The optimal choice of the parameters σ, μ_l and ν in (2.3) is discussed in [9, 10] and is made in order to minimize the error (2.5) of the inverse Laplace approximation formula (2.4).

It follows that the coefficients of the fast methods involve the evaluations of the Laplace transform of the kernel at some suitable points of the complex plane. In the following subsection, we briefly recall the FCOLL and FVRK methods.

2.1. Fast collocation methods. The idea of a collocation method [2] is to approximate the exact solution of (2.1) by a piecewise polynomial function $u(t)$ of the form

$$u(t_n + \theta h) = \sum_{i=1}^m L_i(\theta) Y_{n,i} \quad \theta \in (0, 1] \quad n = 0, \dots, N-1,$$

where $L_i(\theta)$ is the i th Lagrange fundamental polynomial with respect to m fixed collocation parameters $c_i \in [0, 1]$. The unknowns $Y_{n,i}$ are determined by requiring that $u(t)$ exactly satisfies the integral equation in the collocation points $t_{n,i} := t_n + c_i h$. In the case of FCOLL methods [6] such conditions lead to the following linear system

$$(\mathbf{I} - h\mathbf{D})\mathbf{Y}_n = \mathbf{F}_n,$$

where $\mathbf{Y}_n = (Y_{n,1}, \dots, Y_{n,m})^T$, $\mathbf{F}_n = (F_{n,1}, \dots, F_{n,m})^T$ is a numerical approximation of (2.2), \mathbf{I} denotes the identity matrix of order m , and \mathbf{D} is a square matrix of dimension m whose elements are

$$(2.6) \quad d_{is} = B_s \sum_{r=0}^{m-1} \frac{(-1)^{m-1-r} \sigma_{s,m-1-r}}{h^{r+1}} \Psi_{ir}$$

and

$$(2.7) \quad \left\{ \begin{array}{l} B_s = \prod_{\substack{r=1 \\ r \neq s}}^m \frac{1}{c_s - c_r} \\ \sigma_{s,0} = 1, \quad \sigma_{s,i} = \sum_{\substack{n_1 < \dots < n_i = 1 \\ n_k \neq s}}^m c_{n_1} c_{n_2} \dots c_{n_i} \\ \Psi_{il} = \sum_{j=-N_p}^{N_p} \omega_j \frac{l}{\lambda_j^{l+1}} K(\lambda_j) e^{c_i h \lambda_j}. \end{array} \right.$$

Each component of the lag terms approximation vector \mathbf{F}_n is computed in the following way. Let us fix an integer $B > 1$ and let L be the smallest integer for which $t_{n+1} < 2B^L h$. The interval $[0, t_n]$ is split into

$$[0, t_n] = \bigcup_{l=1}^L [\tau_l, \tau_{l-1}],$$

where the mesh points τ_l are of the form $\tau_l = q_l B^L h$ with $q_l \geq 1$ determined by requiring that $\tau_0 = t_n, \tau_L = 0$ and for $l = 1, \dots, L-1, t_{n+1} - \tau_l \in [B^l h, (2B^l - 1)h]$. We choose a different Talbot contour for each interval and we denote by $\omega_j^{(l)}$ and $\lambda_j^{(l)}$ the corresponding weights and nodes in the formula (2.4).

Then we have

$$F_{n,i} = f(t_{n,i}) + \sum_{l=1}^L \sum_{j=-N_p}^{N_p} \omega_j^{(l)} K(\lambda_j^{(l)}) e^{(t_{n,i} - \tau_{l-1})\lambda_j^{(l)}} z(\tau_{l-1}, \tau_l, \lambda_j^{(l)}), \quad i = 1, \dots, m,$$

where

$$z(\tau_{l-1}, \tau_l, \lambda_j^{(l)}) = \int_{\tau_l}^{\tau_{l-1}} e^{(\tau_{l-1} - \tau)\lambda_j^{(l)}} u(\tau) d\tau.$$

In [6] the following convergence theorem has been proved.

THEOREM 2.1. *Let $e(t) = y(t) - u(t)$ be the error of the FCOLL methods. Then*

$$\|e\|_\infty = O(h^m) + O(e^{-c\sqrt{M}})$$

for every choice of the collocation parameters $0 \leq c_1 < \dots < c_m \leq 1$.

REMARK 2.2. It is possible to achieve local superconvergence at the mesh points by opportunely choosing the collocation parameters c_i , and sufficiently large M :

(a) If the collocation parameters are the Radau II points for $(0, 1]$, then we have

$$\max_{t_n \in I_h} |e_n| = O(h^{2m-1}).$$

(b) If the collocation parameters are the Lobatto points for $[0, 1]$, then we obtain

$$\max_{t_n \in I_h} |e_n| = O(h^{2m-2}).$$

(c) If the first $m-1$ collocation parameters are the Gauss points for $(0, 1)$ and $c_m = 1$, then we obtain

$$\max_{t_n \in I_h} |e_n| = O(h^{2m-2}).$$

2.2. Fast Runge–Kutta methods. Runge–Kutta methods for VIEs (VRK methods) [3] are determined by the “Butcher array” for ODEs

$$(2.8) \quad \begin{array}{c|c} \mathbf{c} & \mathbf{A} \\ \hline & \mathbf{b}^T \end{array}$$

where the vectors $\mathbf{b} = (b_i)_{i=1}^m$, $\mathbf{c} = (c_i)_{i=1}^m$ and the matrix $\mathbf{A} = (a_{is})_{i,s=1}^m$ are fixed. Explicit VRK methods of Pouzet type (PVRK methods) are characterized by a strictly lower

triangular matrix \mathbf{A} while implicit VRK methods of de Hoog and Weiss (HVRK methods) are characterized by

$$(2.9) \quad b_k = \int_0^1 L_k(\theta) d\theta, \quad k = 1, \dots, m, \quad a_{is} := \int_0^{c_i} L_s(\theta) d\theta = c_i \sum_{j=1}^m b_j L_s(c_j c_i), \quad c_m = 1.$$

An m -stage FVRK method [4] applied to the equation (2.1) reads

$$y_{n+1} = \begin{cases} F_{n,m+1} + h \sum_{i=1}^m b_i \Phi_i Y_{n,i} & \text{FPVRK methods} \\ Y_{n,m} & \text{FHVRK methods,} \end{cases} \quad n = 0, \dots, N-1,$$

where $\Phi_i = \sum_{j=-N_p}^{N_p} \omega_j K(\lambda_j) e^{(1-c_i)h\lambda_j}$ and the stages $Y_{n,i}$ are computed by solving the linear system

$$(\mathbf{I} - h\mathbf{D})\mathbf{Y}_n = \mathbf{F}_n.$$

Here $\mathbf{Y}_n = (Y_{n,1}, \dots, Y_{n,m})^T$, $\mathbf{F}_n = (F_{n,1}, \dots, F_{n,m})^T$ is a numerical approximation of (2.2), \mathbf{I} denotes the identity matrix of order m , $\mathbf{D} = (d_{is})$ is a square matrix of dimension m whose elements are

$$(2.10) \quad d_{is} = \begin{cases} a_{is} \Psi_{is} & \text{FPVRK methods} \\ c_i \sum_{l=1}^m b_l \Psi_{il} L_s(c_l c_i) & \text{FHVRK methods,} \end{cases}$$

and

$$(2.11) \quad \Psi_{il} = \begin{cases} \sum_{j=-N_p}^{N_p} \omega_j K(\lambda_j) e^{(c_i - c_l)h\lambda_j} & \text{FPVRK methods} \\ \sum_{j=-N_p}^{N_p} \omega_j K(\lambda_j) e^{c_i(1-c_l)h\lambda_j} & \text{FHVRK methods.} \end{cases}$$

The lag term approximation \mathbf{F}_n is the same for FPVRK and FHVRK methods and it is computed through

$$F_{n,i} = f(t_{n,i}) + \sum_{l=1}^L \sum_{j=-N_p}^{N_p} \omega_j^{(l)} K(\lambda_j^{(l)}) e^{(t_{n,i} - \tau_{l-1})\lambda_j^{(l)}} z(\tau_{l-1}, \tau_l, \lambda_j^{(l)}), \quad i = 1, \dots, m,$$

where

$$z(\tau_{l-1}, \tau_l, \lambda_j^{(l)}) := h \sum_{r=\frac{\tau_l}{h}}^{\frac{\tau_{l-1}}{h}-1} \sum_{s=1}^m b_s e^{(\tau_{l-1} - t_{r,s})\lambda_j^{(l)}} g(t_{r,s}, Y_{r,s}),$$

and the points τ_l are the same of those determined for FCOLL methods.

In [4] the following convergence theorem has been proved.

THEOREM 2.3. *Let $\bar{e}_n = y(t_n) - \bar{y}_n$ be the error of the FVRK method. Let p be the order of the corresponding classical VRK method (i.e., having the same Butcher array). Then*

$$\max_{1 \leq n \leq N} |\bar{e}_n| = O(h^p) + O(e^{-c\sqrt{M}}).$$

REMARK 2.4. By choosing implicit FHVRK methods with nodes $\{c_i\}$ as in Remark 2.2, we obtain superconvergent FVRK methods, i.e., $p = 2m - 1$ with m RadauII points, $p = 2m - 2$ with m Lobatto points and $p = 2m - 2$ with $m - 1$ Gauss points and $c_m = 1$.

3. Stability analysis for the basic test equation. In this section we will analyze the stability properties of the fast methods with respect to the basic test equation,

$$(3.1) \quad y(t) = 1 + \mu \int_0^t y(\tau) d\tau, \quad t \in [0, T], \operatorname{Re}(\mu) < 0.$$

Since the exact solution $y(t)$ of (3.1) tends to zero when t goes to $+\infty$, it is natural to require that the numerical solution y_n produced by a numerical method when applied to the equation (3.1) with stepsize h , has the same behaviour. Thus we recall the following definition of numerical stability.

DEFINITION 3.1. A numerical method is said to be stable for given $z := h\mu \in \mathbb{C}$ if the numerical solution y_n , resulting from applying the method to (3.1) with fixed stepsize h , tends to zero when $n \rightarrow +\infty$.

DEFINITION 3.2. The region of absolute stability of the method is the set of all values $z \in \mathbb{C}$ for which the method is stable.

DEFINITION 3.3. The method is said *A-stable* if its region of absolute stability includes the negative complex half plane \mathbb{C}^- .

The application of either a FVRK method (FPVRK and FHVRK method) or a FCOLL method to the equation (3.1), leads to the following linear system,

$$(3.2) \quad (\mathbf{I} - z\mathbf{D})\mathbf{Y}_n = \mathbf{F}_n,$$

where the matrix \mathbf{D} is obtained from (2.10) for FVRK methods and from (2.6) for FCOLL methods with $K(s) = \frac{1}{s}$, and

$$(3.3) \quad \mathbf{F}_n = \mathbf{u} + z \sum_{k=0}^{n-1} \mathbf{Q}_{n,k}^{(l)} \mathbf{Y}_k.$$

Here $\mathbf{u} = (1, \dots, 1)^T$ and $\mathbf{Q}_{n,k}^{(l)}$ is a square matrix of dimension m whose elements are

$$(3.4) \quad \left(\mathbf{Q}_{n,k}^{(l)} \right)_{i,s=1,\dots,m} = \begin{cases} b_s \sum_{j=-N_p}^{N_p} \frac{\omega_j^{(l)}}{\lambda_j^{(l)}} e^{(t_{n,i}-t_{k,s})\lambda_j^{(l)}} & \text{FVRK methods} \\ \sum_{j=-N_p}^{N_p} \frac{\omega_j^{(l)}}{\lambda_j^{(l)}} e^{(t_{n,i}-t_k)\lambda_j^{(l)}} \int_0^1 e^{-\theta h \lambda_j^{(l)}} L_s(\theta) d\theta & \text{FCOLL methods.} \end{cases}$$

The index l in the formula (3.3) is determined by n and k in such a way that $t_k \in [\tau_l, \tau_{l-1}]$.

In the following theorem we provide the expression for the stability matrix of fast methods.

THEOREM 3.4. A fast method applied to the test equation (3.1) leads to the two term relation,

$$(3.5) \quad \mathbf{Y}_n = \mathbf{R}(z)\mathbf{Y}_{n-1},$$

where

$$(3.6) \quad \mathbf{R}(z) = (\mathbf{I} + z(\mathbf{I} - z\mathbf{D})^{-1}\mathbf{Q}_1^{(1)})$$

is a square matrix of dimension m , with $\mathbf{Q}_1^{(1)} = \mathbf{Q}_{n,n-1}^{(1)}$ given by (3.4) and \mathbf{D} defined by (2.6) or (2.10).

Proof. Assuming that $\det(\mathbf{I} - z\mathbf{D}) \neq 0$, the formula (3.2) can be rewritten as

$$(3.7) \quad \mathbf{Y}_n = (\mathbf{I} - z\mathbf{D})^{-1} \left(\mathbf{u} + z \sum_{k=0}^{n-1} \mathbf{Q}_{n,k}^{(l)} \mathbf{Y}_k \right).$$

By subtracting the expressions of \mathbf{Y}_n and \mathbf{Y}_{n-1} given by (3.7) and by opportune manipulations, we obtain, for $n \geq 1$,

$$(3.8) \quad \mathbf{Y}_n = (\mathbf{I} + z(\mathbf{I} - z\mathbf{D})^{-1} \mathbf{Q}_1^{(1)}) \mathbf{Y}_{n-1} + \sum_{k=0}^{n-2} z(\mathbf{I} - z\mathbf{D})^{-1} \left[\mathbf{Q}_{n,k}^{(l)} - \mathbf{Q}_{n-1,k}^{(l)} \right] \mathbf{Y}_k,$$

with

$$\mathbf{Y}_0 = (\mathbf{I} - z\mathbf{D})^{-1} \mathbf{u}.$$

Let us denote with $\check{f}(t)$ the inverse Laplace transform approximation of $\frac{1}{s}$ obtained through the formula (2.4). Then the formula (3.4) can be rewritten as

$$\left(\mathbf{Q}_{n,k}^{(l)} \right)_{i,j} = \begin{cases} b_j \check{f}(t_{n,i} - t_{k,j}) & \text{FVRK methods} \\ \int_0^1 \check{f}(t_{n,i} - t_k - \theta h) L_j(\theta) d\theta & \text{FCOLL methods.} \end{cases}$$

We can freeze the relative error of the inverse Laplace transform approximation $\check{f}(t)$ obtained through the formula (2.4) in the approximation interval, as this error is of order $O(e^{-c\sqrt{M}})$, independently of t . Since the exact inverse Laplace transform of $\frac{1}{s}$ is a constant function, this implies that $\check{f}(t)$ is a constant function, too. It follows that in (3.8) $\mathbf{Q}_{n,k}^{(l)} = \mathbf{Q}_{n-1,k}^{(l)}$ and thus the theorem is proved. \square

The next result is an immediate consequence of Theorem 3.4 and of the Definition 3.

COROLLARY 3.5. *If the eigenvalues of $\mathbf{R}(z)$ are within the unit circle, then the fast method is stable. The region of absolute stability of the method is thus the set*

$$\mathcal{S} = \{z \in \mathbb{C} : |\text{eig}(\mathbf{R}(z))| < 1\}.$$

Note that the stability regions of the fast methods depend on the number of points $M = 2N_p + 1$ chosen for the approximation (2.4). If $M \rightarrow +\infty$, since the fast methods tend to the classical ones, we expect that the same happens for the corresponding stability regions.

THEOREM 3.6. *The stability regions of the fast methods tend, as $M \rightarrow \infty$, to the stability regions of the corresponding classical methods.*

Proof. Let us consider the stability matrix (3.6). If $M \rightarrow \infty$ we have

$$\begin{aligned} \mathbf{Q}_1^{(1)} &\rightarrow \mathbf{u}\mathbf{b}^T \\ \mathbf{D} &\rightarrow \mathbf{A} \end{aligned}$$

where \mathbf{b}^T and \mathbf{A} are given by (2.8) for FPVRK methods and by (2.9) for FHVRK methods. Since we are considering a linear constant kernel, it is easy to check that the vector \mathbf{b}^T and the matrix \mathbf{A} for FCOLL methods are the same as those of FHVRK methods. It immediately follows that

$$\mathbf{R}(z) \rightarrow r(z) := \mathbf{I} + z(\mathbf{I} - z\mathbf{A})^{-1} \mathbf{u}\mathbf{b}^T.$$

This is an $m \times m$ matrix whose eigenvalues are $\lambda_1 = 1 + z\mathbf{b}^T(\mathbf{I} - z\mathbf{A})^{-1}\mathbf{u} = r(z)$ with multiplicity 1 and $\lambda_2 = 1$ with multiplicity $m-1$. Since $\mathbf{Y}_0 = (\mathbf{I} - z\mathbf{D})^{-1}\mathbf{u}$ is an eigenvector associated with the eigenvalue $r(z)$, it follows that the two-term recursion (3.5) of the fast methods tends to

$$\mathbf{Y}_n = r(z)\mathbf{Y}_{n-1}.$$

We observe that the previous formula is the two-term recursion of the classical methods (see [1]), and so the theorem is proved. \square

The following corollary, with fixed number $M = 2N_p + 1$ of points on the Talbot contour, provides a condition on the parameters c_j sufficient for unbounded stability regions.

COROLLARY 3.7. *If the parameters c_j satisfy,*

$$(3.9) \quad |\text{eig}(\mathbf{I} - \mathbf{D}^{-1}\mathbf{Q}_1^{(1)})| < 1,$$

then the stability region of the fast method with respect to equation (3.1) is unbounded.

Proof. From the expression (3.6) for the stability matrix $\mathbf{R}(z)$, we obtain

$$\lim_{|z| \rightarrow -\infty} \mathbf{R}(z) = \mathbf{I} - \mathbf{D}^{-1}\mathbf{Q}_1^{(1)},$$

and thus the theorem follows. \square

We now provide some examples of fast methods which satisfy this condition.

EXAMPLE 3.8. The implicit Euler FHVRK method is characterized by $m = 1$, $c_1 = 1$, $b_1 = 1$, $a_{11} = 1$. The stability matrix is $R(z) = 1 + z(1 - zd_{11})^{-1}Q_1^{(1)}$, where $Q_1^{(1)} = \sum_{j=-N_p}^{N_p} \frac{\omega_j^{(1)}}{\lambda_j^{(1)}} e^{h\lambda_j^{(1)}} =: \beta$ and $d_{11} = c_1 b_1 \Psi_{11} L_1(c_1 c_1) = \Psi_{11} = \sum_{j=-N_p}^{N_p} \frac{\omega_j}{\lambda_j} =: \alpha$. It can immediately be proved that the condition (3.9) is satisfied, since

$$|\mathbf{I} - \mathbf{D}^{-1}\mathbf{Q}_1^{(1)}| = |1 - \frac{\beta}{\alpha}| < 1,$$

so the implicit Euler FHVRK method has an unbounded stability region for all values of M . In fact the stability function is

$$R(z) = 1 + \frac{z\beta}{1 - z\alpha},$$

and an easy computation shows that $|R(z)| < 1$ if and only if z is outside the circle $\mathcal{C}_{\alpha,\beta}$ centered at $C = \left(\frac{1}{2\alpha-\beta}, 0\right)$ with radius $r = \frac{1}{|2\alpha-\beta|}$. Then the implicit Euler FVRK method is A -stable for all values of M , the circle $\mathcal{C}_{\alpha,\beta}$ being entirely contained in the right half of the complex plane. We observe that when $M \rightarrow \infty$, then $\alpha, \beta \rightarrow 1$ and the stability region tends to that of the classical Euler method, that is, the region outside the circle centered in $(1, 0)$ and with radius equal to 1.

EXAMPLE 3.9. We checked that, if we fix $N_p \geq 21$, then the fast midpoint rule (i.e., the 1-point Gauss FHVRK method characterized by $c_1 = \frac{1}{2}$) satisfies the condition (3.9) and thus the stability region is unbounded; see Figure 5.2 in the section of stability plots.

EXAMPLE 3.10. Analogously, we checked that the stability region of the 3-point Radau II FHVRK method ($c_1 = \frac{4-\sqrt{6}}{10}$, $c_2 = \frac{4+\sqrt{6}}{10}$, $c_3 = 1$) is unbounded for any fixed value of N_p .

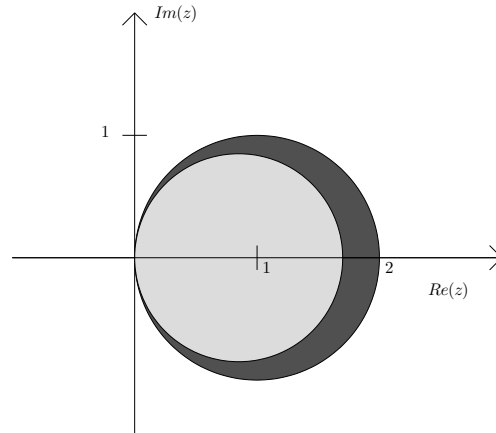


FIG. 3.1. Stability regions of the classical implicit Euler VRK method vs Fast implicit Euler VRK method

4. Stability analysis for the convolution test equation. Now we will study the stability properties of the fast methods with respect to the convolution test equation,

$$(4.1) \quad y(t) = 1 + \int_0^t [\mu + \sigma(t - \tau)]y(\tau)d\tau, \quad t \in [0, T], \quad \mu < 0, \quad \sigma \leq 0.$$

Since the exact solution $y(t)$ of (4.1) goes to zero when $t \rightarrow +\infty$, it is natural to require that the numerical solution y_n , produced by the fast methods when applied to (4.1) with stepsize h , has the same behaviour.

Thus we recall the following definition of numerical stability [3].

DEFINITION 4.1. A numerical method is said to be stable for given $z := h\mu$, $w := h^2\sigma$ if it yields an approximate solution y_n which satisfies $y_n \rightarrow 0$ as $n \rightarrow \infty$ whenever it is applied with a fixed stepsize $h > 0$ to the test equation (4.1).

DEFINITION 4.2. The region of stability of the method is the set of all values (z, w) for which the method is stable.

Let \mathbf{D} and $\tilde{\mathbf{D}}$ be obtained by substituting $K(s) = 1/s$ and $K(s) = 1/s^2$ in (2.6)-(2.7) (FCOLL methods) and in (2.10)-(2.11) (FVRK methods), respectively, and let $\bar{\mathbf{D}} = \tilde{\mathbf{D}}/h$. Then the application of a fast method to the test equation (4.1) leads to

$$(4.2) \quad \mathbf{Y}_n = \mathbf{N}^{-1}\mathbf{F}_n,$$

$$(4.3) \quad \mathbf{F}_n = \mathbf{u} + \sum_{r=0}^{n-1} \left[z\mathbf{Q}_{n,r}^{(l)} + (w(n-r)\mathbf{I} + w\bar{\theta})\bar{\mathbf{Q}}_{n,r}^{(l)} - w\mathbf{P}_{n,r}^{(l)} \right] \mathbf{Y}_r,$$

where the matrices $\mathbf{Q}_{n,r}^{(l)}$ are given by (3.4) and

$$(4.4) \quad \mathbf{N} = \mathbf{I} - z\mathbf{D} - w\bar{\mathbf{D}},$$

$$(4.5) \quad \left(\bar{\mathbf{Q}}_{n,r}^{(l)} \right)_{i,s} = \begin{cases} b_s \sum_{j=-N_p}^{N_p} \frac{\omega_j^{(l)}}{(\lambda_j^{(l)})^2} \frac{e^{(t_{n,i}-t_{r,s})\lambda_j^{(l)}}}{t_{n,i}-t_{r,s}} & \text{FVRK methods} \\ \sum_{j=-N_p}^{N_p} \frac{\omega_j^{(l)}}{(\lambda_j^{(l)})^2} \frac{e^{(t_{n,i}-t_{r,s})\lambda_j^{(l)}}}{t_{n,i}-t_{r,s}} \int_0^1 e^{-\theta h \lambda_j^{(l)}} L_s(\theta) d\theta & \text{FCOLL methods,} \end{cases}$$

$$(4.6) \quad \left(\mathbf{P}_{n,r}^{(l)} \right)_{i,s} = c_s \left(\bar{\mathbf{Q}}_{n,r}^{(l)} \right)_{i,s},$$

$$\bar{\theta} = \text{diag}(c_1, \dots, c_s),$$

are square matrices of dimension m . The index l in the formula (4.3) is determined by n and k in such a way that $t_k \in [\tau_l, \tau_{l-1}]$ and the matrix \mathbf{N} is supposed to be nonsingular.

THEOREM 4.3. *A fast method applied to the test equation (4.1) leads to the following recurrence relation*

$$(4.7) \quad \mathbf{Y}_{n+2} = \mathbf{E}\mathbf{Y}_{n+1} - \mathbf{F}\mathbf{Y}_n,$$

where

$$\begin{aligned} \mathbf{E} &= \mathbf{N}^{-1} \left(\mathbf{N} + w\bar{\mathbf{Q}}_1^{(1)} + \mathbf{S} \right), \\ \mathbf{F} &= -\mathbf{N}^{-1}\mathbf{S}, \\ \mathbf{S} &= \mathbf{N} + z\mathbf{Q}_1^{(1)} + w\bar{\theta}\bar{\mathbf{Q}}_1^{(1)} - w\mathbf{P}_1^{(1)}, \end{aligned}$$

\mathbf{N} is given by (4.4), and $\mathbf{Q}_1^{(1)} = \mathbf{Q}_{n+2,n+1}^{(1)}$, $\bar{\mathbf{Q}}_1^{(1)} = \bar{\mathbf{Q}}_{n+2,n+1}^{(1)}$, $\mathbf{P}_1^{(1)} = \mathbf{P}_{n+2,n+1}^{(1)}$ are given by (3.4), (4.5), (4.6)

Proof. From (4.2) and (4.3) it is possible to obtain the relation

$$(4.8) \quad \begin{aligned} \mathbf{N}\mathbf{Y}_{n+2} &= \left(\mathbf{N} + w\bar{\mathbf{Q}}_1^{(1)} + \mathbf{S} \right) \mathbf{Y}_{n+1} - \left(\mathbf{S} - \mathbf{T}_{n+2,n}^{(l)} \right) \mathbf{Y}_n \\ &\quad + \sum_{r=0}^{n-1} \left(\mathbf{T}_{n+2,r}^{(l)} - \mathbf{T}_{n+1,r}^{(l)} + w\Delta\mathbf{Q}_{n+1,r}^{(l)} \right) \mathbf{Y}_r, \end{aligned}$$

where

$$\begin{aligned} \Delta\mathbf{Q}_{n,r}^{(l)} &= \mathbf{Q}_{n,r}^{(l)} - \mathbf{Q}_{n-1,r}^{(l)}, & \Delta\bar{\mathbf{Q}}_{n,r}^{(l)} &= \bar{\mathbf{Q}}_{n,r}^{(l)} - \bar{\mathbf{Q}}_{n-1,r}^{(l)}, \\ \Delta\mathbf{P}_{n,r}^{(l)} &= \mathbf{P}_{n,r}^{(l)} - \mathbf{P}_{n-1,r}^{(l)}, \\ \mathbf{T}_{n,r}^{(l)} &= z\Delta\mathbf{Q}_{n,r}^{(l)} + [w(n-r)\mathbf{I} + w\bar{\theta}] \Delta\bar{\mathbf{Q}}_{n,r}^{(l)} - w\Delta\mathbf{P}_{n,r}^{(l)}, \end{aligned}$$

and $\mathbf{Q}_{n,r}^{(l)}$, $\bar{\mathbf{Q}}_{n,r}^{(l)}$, $\mathbf{P}_{n,r}^{(l)}$ are given by (3.4), (4.5), (4.6).

As in Section 3, by freezing the relative error of the inverse Laplace transform approximation, it follows that $\mathbf{Q}_{n,r}^{(l)} = \mathbf{Q}_{n-1,r}^{(l)}$. Similarly we obtain that $\bar{\mathbf{Q}}_{n,r}^{(l)} = \bar{\mathbf{Q}}_{n-1,r}^{(l)}$ and $\mathbf{P}_{n,r}^{(l)} = \mathbf{P}_{n-1,r}^{(l)}$. Thus the relation (4.8) becomes a difference equation of fixed order and the theorem is proved. \square

The relation (4.7) can be written in the form

$$(4.9) \quad \begin{bmatrix} \mathbf{Y}_{n+1} \\ \mathbf{Y}_n \end{bmatrix} = \mathbf{R}(z, w) \begin{bmatrix} \mathbf{Y}_n \\ \mathbf{Y}_{n-1} \end{bmatrix},$$

for $n = 1, 2, \dots$, where

$$(4.10) \quad \mathbf{R}(z, w) = \begin{bmatrix} \mathbf{E} & \mathbf{F} \\ \mathbf{I} & \mathbf{0} \end{bmatrix}.$$

The next result immediately follows from relations (4.9)-(4.10) and from the Definition 4.2.

COROLLARY 4.4. *If the eigenvalues of $\mathbf{R}(z, w)$ are within the unit circle, then the fast method is stable. The stability region of the method is thus the set*

$$\mathcal{S} = \{(z, w) \in \mathbb{R}_- \times \mathbb{R}_- : |\text{eig}(\mathbf{R}(z, w))| < 1\}.$$

As was proven in Theorem 3.6 for the basic test equation, in the case of the convolution test equation we are also able to prove that

THEOREM 4.5. *The stability regions of the fast methods tend, as $M \rightarrow \infty$, to the stability regions of the corresponding classical ones.*

Proof. The proof is analogous to that of Theorem 3.6 and it is obtained by proving that the three term recursion (4.7) tends to the three term recursion of classical methods [1]. \square

REMARK 4.6. In the case $\sigma = 0$ the region of absolute stability of a fast method with respect to the test equation (4.1), given by Corollary 4.4, reduces to the interval of absolute stability of the fast method with respect to equation (3.1).

REMARK 4.7. As a consequence of Corollary 3.7, it follows that, for any fixed N_p , if the parameters c_j satisfy the condition (3.9), then the corresponding fast methods are characterized by unbounded stability regions with respect to equation (4.1) along the z -axis.

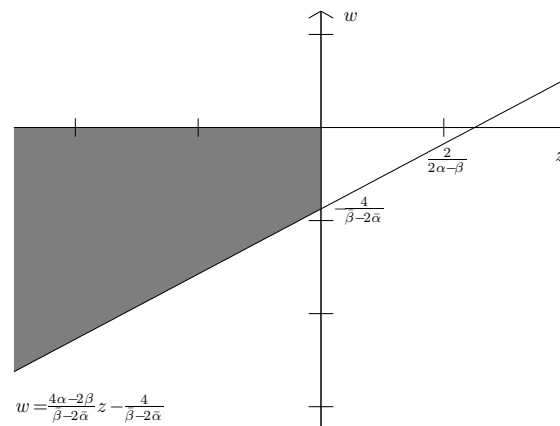


FIG. 4.1. Stability region of the implicit Euler FVRK method

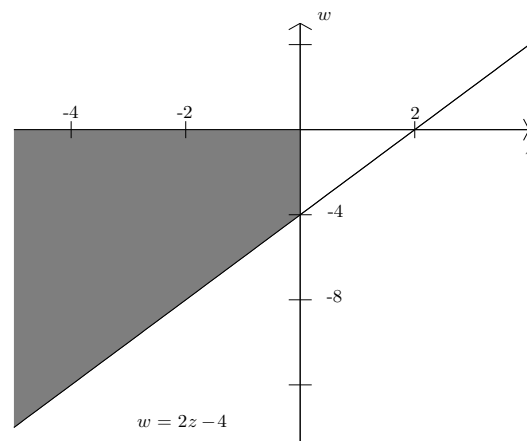


FIG. 4.2. Stability region of the classical implicit Euler VRK method

EXAMPLE 4.8. Let us consider the implicit Euler FVRK method characterized by $m = 1$, $c_1 = 1$, $b_1 = 1$, $a_{11} = 1$. As we proved in Example 3.8, the condition (3.9) is satisfied for any fixed value of N_p , then it follows from Remark 4.7 that the stability region

of implicit Euler FVRK method with respect to equation (4.1) is unbounded along the z -axis. In this case we have

$$\begin{aligned}
 d_{11} &= c_1 b_1 \Psi_{11} L_1(c_1 c_1) = \Psi_{11} = \sum_{j=-N_p}^{N_p} \frac{\omega_j}{\lambda_j} =: \alpha \\
 \bar{d}_{11} &= c_1 b_1 \bar{\Psi}_{11} L_1(c_1 c_1) = \bar{\Psi}_{11} = \sum_{j=-N_p}^{N_p} \frac{\omega_j}{h(\lambda_j)^2} =: \bar{\alpha} \\
 Q_1^{(1)} &= \sum_{j=-N_p}^{N_p} \frac{\omega_j^{(1)}}{\lambda_j^{(1)}} e^{h\lambda_j^{(1)}} =: \beta \\
 \bar{Q}_1^{(1)} &= \sum_{j=-N_p}^{N_p} \frac{\omega_j^{(1)}}{(\lambda_j^{(1)})^2} \frac{e^{h\lambda_j^{(1)}}}{h} =: \bar{\beta} \\
 P_1^{(1)} &= \bar{Q}_1^{(1)} = \bar{\beta} \\
 N &= 1 - \alpha z - \bar{\alpha} w,
 \end{aligned}$$

from which it follows that

$$\mathbf{S} = \begin{bmatrix} \frac{(\beta-2\alpha)z+(\bar{\beta}-2\bar{\alpha})w+2}{1-\alpha z-\bar{\alpha}w} & -\frac{(\beta-\alpha)z+\bar{\alpha}w+1}{1-\alpha z-\bar{\alpha}w} \\ 1 & 0 \end{bmatrix}.$$

An easy computation shows that $|\text{eig}(\mathbf{S})| < 1$ if and only if

$$w > \frac{4\alpha - 2\beta}{\bar{\beta} - 2\bar{\alpha}} z - \frac{4}{\bar{\beta} - 2\bar{\alpha}}$$

and the stability region is shown in Figure 4.1. We can observe that when $M \rightarrow \infty$ then $\alpha, \beta, \bar{\beta} \rightarrow 1, \bar{\alpha} \rightarrow 0$, and the stability region tends to that of classical Euler method, that is, the region characterized by

$$w > 2z - 4$$

and represented in Figure 4.2.

EXAMPLE 4.9. As we observed in Example 3.9, if we fix $N_p \geq 21$, then the fast midpoint rule satisfies the condition (3.9) and thus the stability region with respect to equation (4.1) is unbounded along the z -axis.

EXAMPLE 4.10. We checked that the stability region of the 3-point Radau II FHVRK method is unbounded along the z -axis for any fixed value of N_p ; see Figure 5.4 in the section of stability plots.

5. Stability plots. In this section, we report the stability regions of two methods (one explicit and one implicit) with respect to the basic test equation (3.1) and two methods with respect to the convolution test equation (4.1).

In Figures 5.1 and 5.2 we report the stability regions, with respect to the basic test equation, respectively of the 3-points III order Heun FPVRK method whose Butcher array is

$$\begin{array}{c|ccc}
 0 & 0 & 0 & 0 \\
 1/3 & 1/3 & 0 & 0 \\
 2/3 & 0 & 2/3 & 0 \\
 \hline
 & 1/4 & 0 & 3/4
 \end{array}$$

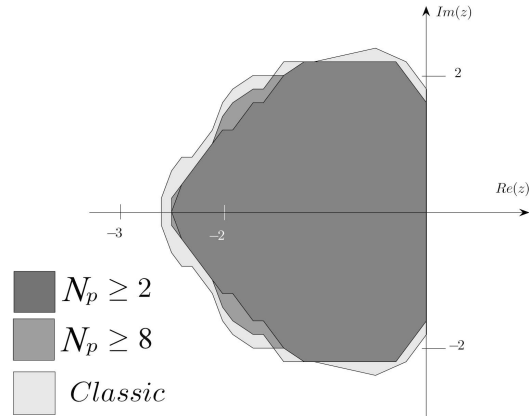


FIG. 5.1. Stability regions of the 3-points Heun method (Fast with $N_p = 2, 8$ and Classic) with respect to equation (3.1).

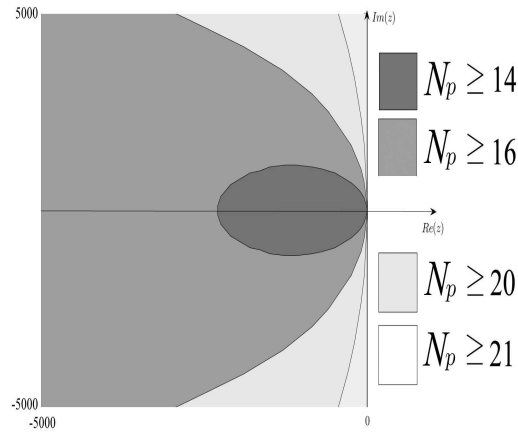


FIG. 5.2. Stability regions of the midpoint rule (Fast with $N_p = 14, 18, 20, 21 = \text{Classic}$) with respect to equation (3.1).

and of the fast midpoint rule, characterized by $c_1 = \frac{1}{2}$.

In Figures 5.3 and 5.4, we report the plots of the stability regions, with respect to the convolution test equation, of an explicit and an implicit method, respectively. Namely, we consider the 4-points IV order FPVRK method whose Butcher array is

$$\begin{array}{c|cccc}
 0 & 0 & 0 & 0 & 0 \\
 1/2 & 1/2 & 0 & 0 & 0 \\
 1/2 & 0 & 1/2 & 0 & 0 \\
 1 & 0 & 0 & 1 & 0 \\
 \hline
 & 1/6 & 1/3 & 1/3 & 1/6
 \end{array}$$

and the the 3-points Radau II FHVRK method characterized by $c_1 = \frac{4-\sqrt{6}}{10}$, $c_2 = \frac{4+\sqrt{6}}{10}$, $c_3 = 1$.

For all plots we report the stability regions of the fast methods at different values of N_p

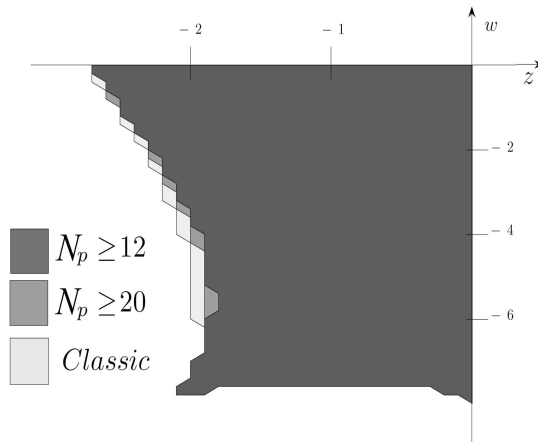


FIG. 5.3. Stability regions of the 4-points IV order FPVRK method (Fast with $N_p = 12, 20$ and Classic) with respect to equation (4.1).

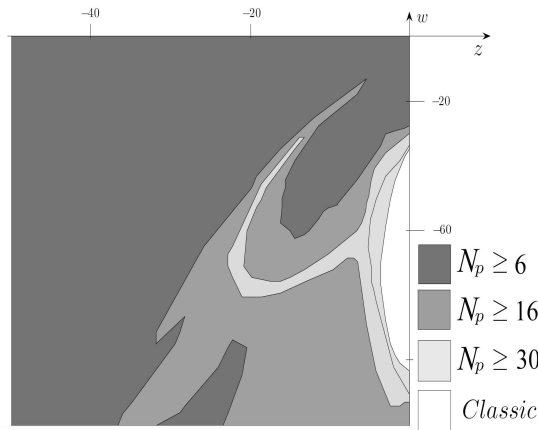


FIG. 5.4. Stability regions of the 3-points Radau II method (Fast with $N_p = 6, 16, 30$ and Classic) with respect to equation (4.1).

and of the classical methods.

The plots show as for the explicit methods the regions of the classical methods are straightway reached for very small values of N_p . The same occurs for all other explicit methods we have tested. As regards the implicit methods, we can observe that this value of N_p is generally larger than for explicit methods, however it remains not very large.

Numerical experiments have been carried out in order to test the reliability of the stability conditions in nonlinear problems. We report the results obtained on the following two-parameters class of VIEs,

$$(5.1) \quad y(t) = 1 - a + ae^{-t} - bt + \int_0^t (b + ae^{-(t-\tau)}) y^2(\tau) d\tau, \quad t \in [0, 30],$$

whose exact solution is $y(t) \equiv 1$. By following a customary approach, we compare the results obtained by our methods on the nonlinear equation (5.1) with the theoretical stability regions

found by a linearized version of the equation. To this end we integrate the equation (5.1) with the following parameters.

Problem	a	b
A	75	-82.5
B	37.5	-45
C	100	-102.5
D	0.16	-2.66

Then, (see [3, p. 457]), we consider the linear expansion in Taylor series of the partial derivative of the kernel $k(t - \tau, y(\tau)) := (b + ae^{-(t-\tau)})y^2(\tau)$ with respect to y , obtaining

$$(5.3) \quad \frac{\partial k(t - \tau, y(\tau))}{\partial y} \simeq [2(a + b) - 2a(t - \tau)]y(\tau).$$

This means we integrate the convolution test equation (4.1) with the following parameters.

Problem	$\mu = 2(a + b)$	$\sigma = -2a$
A	-15	-150
B	-15	-75
C	-5	-200
D	-5	-0.32

In this way, beginning with a stepsize $h = 0.1$ and doubling it from time to time, we move into the $(h\mu, h^2\sigma)$ plane, along the parabolas having curvatures $\frac{\sigma}{\mu^2}$, from the inside to the outside of the theoretical stability regions.

We report in Table 5.1 and in Figures 5.5–5.6 some results obtained by applying, with the different stepsize h , the 4-points IV order FPVRK method (which we call E4) and the implicit Euler FVRK method to the problems (5.2).

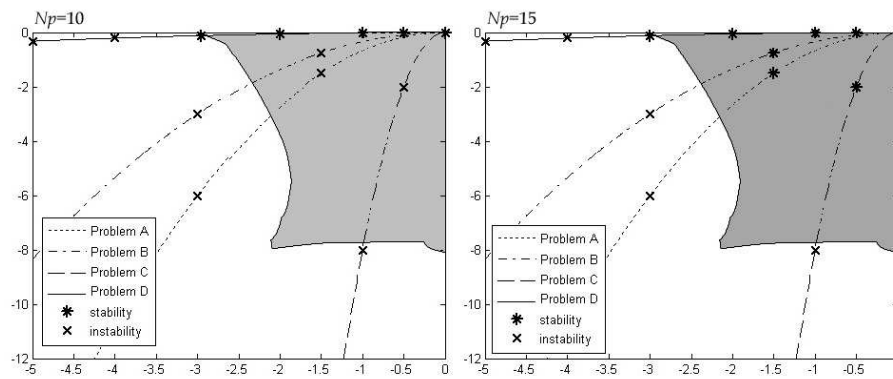


FIG. 5.5. Plots with different h in the plane $(h\mu, h^2\sigma)$ of stable and instable results for the 4-points IV order FPVRK method with $N_p = 10$ and $N_p = 15$ on the problems (5.2).

In the figures we emphasize with ‘*’ or ‘x’ the points $(h\mu, h^2\sigma)$ for the h listed in the second column of the Table 5.1.

The table and the figures confirm how the stability of the methods depends on the choice of the parameters a and b , on the stepsize h , and on the number $M = 2N_p + 1$ of points on the Talbot contour. In fact, we can observe, by varying a and b , how the points $(h\mu, h^2\sigma)$ fall or not into the theoretical stability regions (gray coloured in the figures) and how the methods

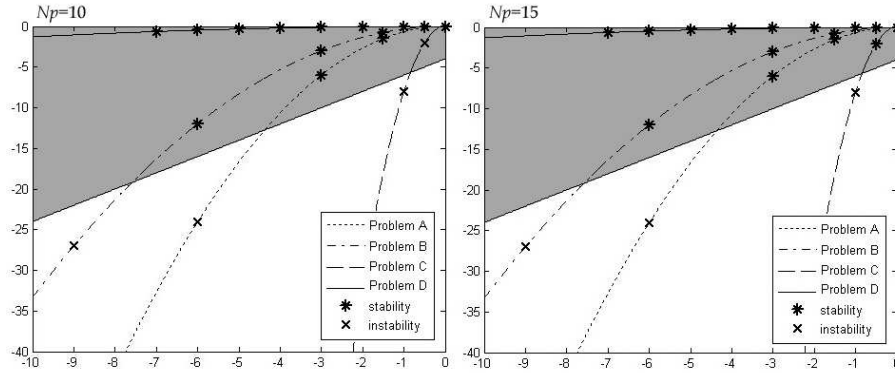


FIG. 5.6. Plots with different h in the plane $(h\mu, h^2\sigma)$ of stable and instable results for the implicit Euler FVRK method with $N_p = 10$ and $N_p = 15$ on the problems (5.2).

on the nonlinear problem (5.1) are stable if we increase N_p . In particular, for the Implicit Euler method the problems A, B and D are well solved (* in Figure 5.6) when $(h\mu, h^2\sigma)$ are inside the stability regions already with $N_p = 10$; the equation C shows stability problems (x in the left Figure 5.6) with $h = 0.1$ when the fast method is run with $N_p = 10$, but it is well solved once N_p increases to 15. For the IV order FPVRK method, the dependence from N_p is more pronounced. In fact, the problems A, B and C show instability for $(h\mu, h^2\sigma)$ with $h = 0.1$ inside the theoretical stability regions when $N_p = 10$ (x in the Figure to left in 5.5), but it's sufficient to increase N_p to 15 and the stability is reached (* in the Figure to right in 5.5).

6. Concluding remarks. In this paper we analyze the stability properties of two classes of numerical methods for Volterra integral equations of Hammerstein type, namely, fast collocation and fast Runge-Kutta methods. The detailed construction of the methods and the results on the computational cost and convergence are reported in [6] and [4]. These fast methods are based on the inverse Laplace transform approximation formula introduced in [9] that allows us to reduce drastically the computational cost of the methods preserving good convergence properties. Here the stability analysis of the two classes of methods is carried out with respect the basic test equation (3.1) and the convolution test equation (4.1). We proved that the stability properties depend on the number $M = 2N_p + 1$ of points chosen on the Talbot contour. In particular for fixed N_p we found the stability matrix for both classes of methods and we determined a condition that provides methods with unbounded stability regions. Moreover we showed that Euler method is A-stable for each value of N_p , while the midpoint rule is A-stable for $N_p \geq 21$. We have done also some experimental tests on a class of nonlinear problems and they confirm the theoretical results.

We recall that in the specialized literature there are some papers on other antitransformation techniques and improvements of Talbot's approximation; see, for example, [8, 13, 14, 15]. In the paper [11], Lubich and his collaborators have already constructed numerical methods for VIEs based on the inverse Laplace Transform approximation introduced in the paper [8]. It would be an interesting topic for future work to study the possibility of constructing numerical methods for VIEs based on other fast antitransformation techniques [13, 14, 15], in order to analyze how the reduction of the error of the inverse Laplace transform approximation formulas influences the performance of the methods.

TABLE 5.1
 Numerical results on problems (5.2).

Problem	h	$2(a+b)h$	$-2ah^2$	N_p	Abs.Err. Euler	in/ out	Abs.Err. E4	in/ out
A	0.1	-1.5	-1.5	10	2.80E-04	in	NaN	in
				15	5.11E-05		2.56E-02	
	0.2	-3	-6	10	3.43E-05	in	NaN	out
				15	5.24E-05		NaN	
B	0.1	-1.5	-0.75	10	7.46E-06	in	NaN	in
				15	2.10E-05		1.96E-02	
	0.2	-3	-3	10	8.73E-05	in	NaN	out
				15	1.90E-05		NaN	
C	0.1	-0.5	-2	10	3.00E+00	in	NaN	in
				15	2.80E-03		7.58E-04	
	0.2	-1	-8	10	2.00E+00	out	NaN	out
				15	2.00E+00		NaN	
D	0.1	-0.5	-0.003225	10	6.60E-06	in	2.11E-05	in
				15	4.76E-05		2.73E-05	
	0.2	-1	-0.0129	10	1.75E-04	in	1.42E-04	in
				15	1.31E-05		9.99E-05	
	0.4	-2	-0.0516	10	4.09E-04	in	7.45E-03	in
				15	6.57E-06		5.15E-03	
	0.6	-3	-0.1161	10	7.90E-04	in	9.36E-02	in
				15	3.69E-05		9.16E-02	
0.8	-4	-0.2064	10	1.85E-08	in	2.04E-01	in	
			15	1.03E-11		1.89E-01		
1.0	-5	-0.3225	10	2.84E-08	in	NaN	out	
			15	3.87E-12		NaN		
1.2	-6	-0.4644	10	1.72E-08	in	-	out	
			15	4.03E-11		-		
1.4	-7	-0.6321	10	2.51E-08	in	-	out	
			15	1.08E-11		-		

REFERENCES

- [1] A. BELLEN, Z. JACKIEWICZ, R. VERMIGLIO, AND M. ZENNARO, *Stability analysis of Runge-Kutta methods for Volterra integral equations of second kind*, IMA J. Numer. Anal., 10 (1990), pp. 103–118.
- [2] H. BRUNNER, *Collocation Methods for Volterra Integral and Related Functional Equations*, Cambridge University Press, Cambridge, 2004.
- [3] H. BRUNNER AND P. J. VAN DER HOUWEN, *The Numerical Solution of Volterra Equations*, CWI Monographs, Vol. 3, North-Holland, Amsterdam, 1986.
- [4] G. CAPOBIANCO, D. CONTE, I. DEL PRETE, AND E. RUSSO, *Fast Runge-Kutta Methods for nonlinear convolution systems of Volterra integral equations*, BIT, 47 (2007), pp. 259–275.

- [5] M. R. CRISCI, E. RUSSO, AND A. VECCHIO, *Stability analysis of the de Hoog and Weiss implicit Runge-Kutta methods for Volterra integro and integro-differential equations*, BIT, 29 (1989), pp. 258–269.
- [6] D. CONTE AND I. DEL PRETE *Fast collocation methods for Volterra integral equations of convolution type*, J. Comput. Appl. Math., 196 (2006), pp. 652–663.
- [7] G. GRIPENBERG, S. O. LONDEN, AND O. STAFFANS, *Volterra Integral and Functional Equations*, Cambridge University Press, Cambridge, 1990.
- [8] M. LÓPEZ-FERNÁNDEZ AND C. PALENCIA, *On the numerical inversion of the Laplace transform of certain holomorphic mappings*, Appl. Numer. Math., 51 (2004), pp. 289–303.
- [9] CH. LUBICH AND A. SCHÄDLE, *Fast convolution for non-reflecting boundary conditions*, SIAM J. Sci. Comput., 24 (2002), pp. 161–182.
- [10] M. RIZZARDI, *A modification of Talbot’s method for the simultaneous approximation of several values of the inverse Laplace transform*, ACM Trans. Math. Software, 21 (1995), pp. 347–371.
- [11] A. SCHÄDLE, M. LÓPEZ-FERNÁNDEZ, AND CH. LUBICH, *Fast and oblivious convolution quadrature*, SIAM J. Sci. Comput., 28 (2006), pp. 421–438.
- [12] A. TALBOT, *The accurate numerical inversion of Laplace transforms*, J. Inst. Math. Appl., 23 (1979), pp. 97–120.
- [13] L. N. TREFETHEN, J. A. C. WEIDEMAN, AND T. SCHMELZER, *Talbot quadratures and rational approximations*, BIT, 46 (2006), pp. 653–670.
- [14] J. A. C. WEIDEMAN, *Optimizing Talbot’s contours for the inversion of the Laplace transform*, SIAM J. Numer. Anal., 44 (2006), pp. 2342–2362.
- [15] J. A. C. WEIDEMAN AND L. N. TREFETHEN, *Parabolic and hyperbolic contours for computing the Bromwich integral*, Math. Comp., 76 (2007), pp. 1341–1356.